

See discussions, stats, and author profiles for this publication at: <https://www.researchgate.net/publication/231661132>

# Spectroscopy and Photophysics of Tetraalkyldibenzoporphycenes

ARTICLE *in* THE JOURNAL OF PHYSICAL CHEMISTRY A · JUNE 1998

Impact Factor: 2.69 · DOI: 10.1021/jp973436i

---

CITATIONS

28

---

READS

6

5 AUTHORS, INCLUDING:



**A. S. Starukhin**

National Academy of Sciences of Belarus

76 PUBLICATIONS 493 CITATIONS

SEE PROFILE



**J. Waluk**

Polish Academy of Sciences

256 PUBLICATIONS 3,683 CITATIONS

SEE PROFILE

## ARTICLES

## Spectroscopy and Photophysics of Tetraalkyldibenzoporphycenes

Jacek Dobkowski,<sup>†</sup> Victor Galievsky,<sup>†,1</sup> Alexander Starukhin,<sup>†,1</sup> Emanuel Vogel,<sup>‡</sup> and Jacek Waluk<sup>\*,†</sup>

*Institute of Physical Chemistry, Polish Academy of Sciences, Kasprzaka 44/52, 01-224 Warsaw, Poland, and Institut für Organische Chemie der Universität, Greinstrasse 4, D-50939 Köln, Germany*

*Received: October 23, 1997; In Final Form: March 26, 1998*

Two recently synthesized derivatives of porphycene, 2,7,12,17-tetramethyl-3,6-13,16-dibenzo[*cde,mno*]-porphycene and 2,7,12,17-tetra-*tert*-butyl-3,6-13,16-dibenzo[*cde,mno*]-porphycene, were studied by stationary and time-resolved spectroscopy and quantum chemical calculations. Both compounds were found to be nonluminescent even at low temperatures. Picosecond transient absorption studies performed in solution at 293 K and in solid nitrogen matrices at 15 K revealed a rapid recovery of the ground-state bleaching. The rate of this process remains very high even at low temperatures. Possible reasons for this photophysical behavior are discussed, including nonplanarity and a fast excited-state *cis*–*trans* NH tautomerization. Electronic transitions of dibenzoporphycenes may be correlated with those of porphyrin and porphycene. However, an “intruder” state lies between the analogues of the Q and Soret bands.

## Introduction

The synthesis of porphycene—the first tetrapyrrolic isomer of porphyrin—and its derivatives initiated intense studies of the chemical and spectral properties of this new class of compounds.<sup>1–9</sup> Comparison of the isomer with porphyrin revealed both similarities and differences. For instance, NMR results proved that *cis* and *trans* NH tautomers are present in the ground state of solid porphycene,<sup>9</sup> whereas in porphyrin only the latter form is observed. A rapid double proton transfer has been detected in the lowest excited singlet state of porphycene,<sup>4,5</sup> while in porphyrin such a process occurs with a low efficiency and involves either a triplet or a hot ground state.<sup>10</sup> The basic pattern of the electronic spectra is similar for the two compounds: two weaker transitions observed in the red portion of the visible region are followed by two strong bands in the UV range. However, significant differences are noticed in regard to the intensity ratio of the visible to the UV bands, energy separation of the two lowest transitions, or the magnetic circular dichroism parameters.<sup>11</sup> The importance of spectral studies is not purely academic: porphycene has already been shown to be a very promising compound in photodynamic therapy.<sup>6</sup>

In this work, we investigate the spectroscopy and photophysics of two recently synthesized derivatives of porphycene, 2,7,12,17-tetramethyl-3,6-13,16-dibenzo[*cde,mno*]-porphycene (**1**) and 2,7,12,17-tetra-*tert*-butyl-3,6-13,16-dibenzo[*cde,mno*]-porphycene (**2**). The first goal of this study was to follow the spectral changes caused by the addition of two ethylene bridges into the porphycene skeleton. In particular, it seemed interesting to find out whether the spectral properties can still be interpreted

by analogy to the parent porphycene chromophore. The second purpose was to look for presence of *cis* and *trans* tautomeric species (Chart 1). The possibility of the presence of both forms was suggested by a very small distance between the nitrogen atoms<sup>12</sup> (2.49 Å in **1** and 2.51 Å in **2**, compared with 2.63 Å in porphycene<sup>2</sup>). For such a small N–N separation, a third form can also be envisaged: a symmetrical structure with inner protons lying halfway between two nitrogen atoms.

## Experimental and computational procedures

The synthesis and purification of **1** and **2** were described elsewhere.<sup>12</sup> Absorption spectra were recorded on a Shimadzu UV 3100 spectrophotometer, equipped with a Beckmann attachment for variable-temperature measurements. Attempts to register fluorescence were made with a Jasný spectrofluorometer.<sup>13</sup> All solvents used were of spectral grade.

For transient picosecond studies, a home-built picosecond spectrometer, described in detail previously,<sup>14</sup> was used. A mode-locked Nd<sup>3+</sup>:YAG laser (EKSMA/EKSPLA) produced pulses of 25 ps fwhm, which were then amplified, and the third harmonic (355 nm) was used to excite the sample. The picosecond continuum, generated in D<sub>2</sub>O by the beam of fundamental frequency and delayed with respect to the excitation beam, was used as a probe. The transmitted pulses were spectrally resolved and detected by photodiode array polychromators.

The cryogenic matrices were prepared using a closed-cycle two-stage Displex 202 (Air Products) refrigerator. The compounds, heated to about 413 K, were mixed with the stream of nitrogen and deposited onto the sapphire window attached to the cold finger (15 K) of the cryostat. The background pressure was 10<sup>–6</sup> Torr.

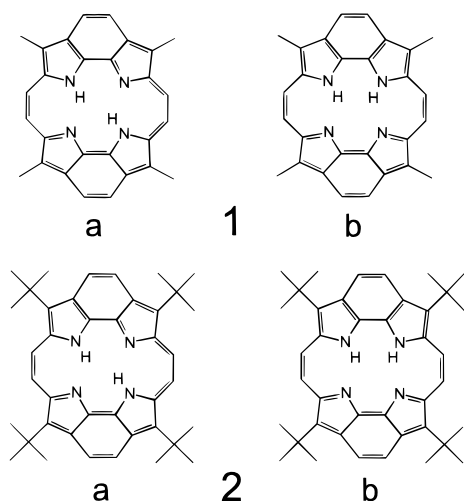
Ground-state geometry optimizations were performed for both the *trans* and *cis* tautomeric forms of **1** and **2** using either

\* To whom correspondence should be addressed. E-mail: waluk@ichf.edu.pl. Fax: (+48) 391 20 238.

<sup>†</sup> Polish Academy of Sciences.

<sup>‡</sup> Institut für Organische Chemie der Universität.

**CHART 1: Trans (a) and Cis (b) Tautomeric Forms of 2,7,12,17-Tetramethyl-3,6-13,16-dibenzo[*cde,mno*]-porphycene (1) and 2,7,12,17-Tetra-*tert*-butyl-3,6-13,16-dibenzo[*cde,mno*]porphycene (2)**



molecular mechanics (MMX force field, PCMODEL<sup>15</sup>) or the PM3 method.<sup>16</sup> For the latter, the UHF formalism was chosen, since the RHF procedure yielded a distorted geometry of the parent porphycene (a similar phenomenon was reported also for porphyrin<sup>17</sup>). The resulting geometry was used in the input for the calculations of excited-state properties. Calculations were also performed using the crystal geometry,<sup>12</sup> “bowl-shaped” for **1**, planar for **2**. Excited-state energies were computed using the INDO/S method,<sup>18</sup> with up to 460 singly excited configurations taken into account in the CI procedure.

## Results and Discussion

Figure 1 shows the room-temperature absorption spectra of **1** and **2** in solvents of varying polarity. The spectra of both compounds are very similar. Two moderately strong electronic transitions, located around 13 000 and 17 000  $\text{cm}^{-1}$ , respectively, may be distinguished in the visible range. On the red edge of absorption, at around 11 000  $\text{cm}^{-1}$ , a weak shoulder is observed. Its intensity does not decrease upon lowering of temperature (Figure 2). Therefore, it cannot be attributed to a hot band. We assign this feature to a separate electronic transition, in agreement with the results of calculations (*vide infra*). In the UV region, a strong, broad band is observed at around 27 000  $\text{cm}^{-1}$ , evidently consisting of several transitions.

The correlation of such a spectral pattern with the one observed in porphycene is not straightforward. Although porphycene and porphyrin reveal similar absorption features—the sequence of two Q transitions in the visible region and two Soret transitions in the near-UV—in **1** and **2** at least three electronic transitions are detected in the visible range. The spacing between the two stronger bands, located around 13 000 and 17 000  $\text{cm}^{-1}$ , respectively, is much larger than in porphycene, where the Q bands are separated by less than 1000  $\text{cm}^{-1}$ . In turn, the gap between the first and the second electronic transitions (the former originating at around 11 000  $\text{cm}^{-1}$ , the latter with a maximum around 13 000  $\text{cm}^{-1}$ ) is about 1000–2000  $\text{cm}^{-1}$ , but if these two transitions are treated as analogues of the Q bands, then the intensity ratio is very different from that observed in porphycene. In any case, there is an “intruder” state in the low-energy region. As discussed below, its presence is correctly predicted by calculations.

The absorption spectra of both compounds are practically insensitive to the solvent polarity. This indicates that one

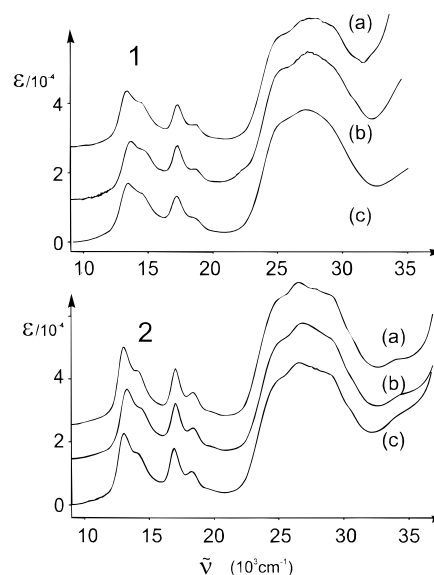


**Figure 1.** Absorption spectra at 293 K: (top) **1** in *n*-hexane (a), acetonitrile (b), and tetrahydrofuran (c); (bottom) **2** in *n*-hexane (a), acetonitrile (b), and *n*-propanol (c). The ordinate scale refers to the lowest traces. Curves a and b have been shifted along the y axes.

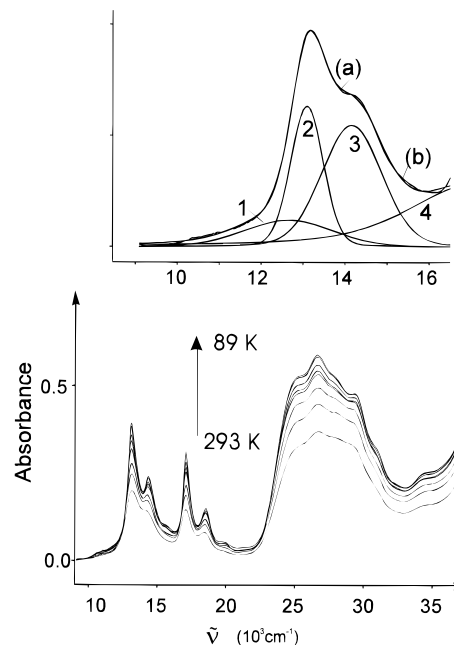


**Figure 2.** (Bottom) Absorption spectra of **2** in EPA (ethyl ether/isopentane/ethanol 5:5:2) recorded as a function of temperature: 293, 243, 213, 173, 143, 113, 91, and 89 K. (Top) Numerical resolution of the low-energy part of the absorption spectrum at 293 K (curve a) into four bands. Curve b is the result of the fit.

tautomeric form is dominant in the ground state. Most probably it is the *trans* tautomer, a form that should have a smaller dipole moment (or no dipole moment at all if the structure is planar).

Figure 2 presents the absorption of **2** recorded as a function of temperature. Except for a sharpening of some peaks and the overall intensity increase due to larger concentration at lower temperatures, no changes are observed in the spectrum upon changing the temperature from 293 to 89 K. This again points to the presence of only one form.

Both compounds revealed no fluorescence, neither at 293 K, nor even at liquid nitrogen temperature. Considering the sensitivity of our instrument, the upper limit for the fluorescence quantum yield may be estimated as  $10^{-4}$ . Lack of fluorescence

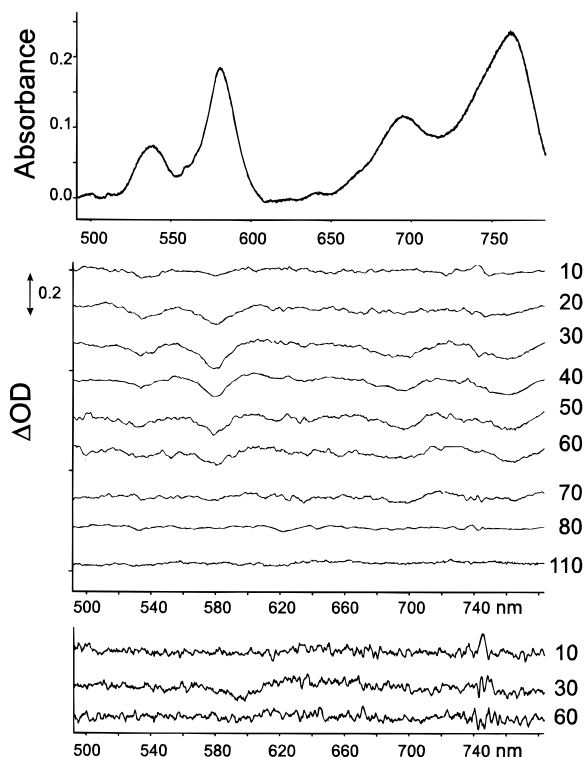


**Figure 3.** (Top) stationary absorption; (middle) picosecond transient absorption of **2** in a nitrogen matrix at 15 K; (bottom) transient absorption in tetrahydrofuran at 293 K. The numbers on the right indicate the delay in picoseconds. The samples were excited at 355 nm.

is in sharp contrast to porphycene and its alkyl derivatives, which either show strong emission already at room temperature or recover the radiative properties as the temperature is lowered.

To determine the nature of the radiationless process responsible for the fast depopulation of the lowest excited singlet state, transient picosecond absorption was measured in the visible range. Room temperature solutions showed a very weak bleaching of the ground-state absorption, which lasted only for several tens of picoseconds (see Figure 3). After that, recovery of the ground state was complete: no longer-lived species was detected.

Essentially the same behavior was observed for low-temperature samples. Figure 3 shows the results of transient absorption measurements performed at 15 K for **2** deposited in a nitrogen matrix. Very fast recovery of the ground state may be seen. The temporal resolution of the instrument is about 30 ps; one can estimate that the ground-state repopulation takes no longer than this value.

Thus, the photophysics of the lowest excited singlet state of **1** and **2** is governed by a very fast temperature-independent internal conversion process, the rate of which is larger than  $3 \times 10^{10} \text{ s}^{-1}$ . Assuming the rate of intersystem crossing similar to that of porphyrin and porphycene, i.e., about  $10^8 \text{ s}^{-1}$ , leads to the estimated triplet formation efficiency lower than 1%. This explains why no population of the triplet state is observed. Lack of fluorescence, in turn, provides another argument for the assignment of the lowest excited singlet state to the weak band observed on the absorption red edge. We have estimated the  $S_1$  radiative rate constant using the Strickler–Berg formula.<sup>19</sup> Two cases were considered. First, the whole absorption curve was integrated between 9000 and 16 000  $\text{cm}^{-1}$ , yielding  $k_r = 1.1 \times 10^8 \text{ s}^{-1}$ . Next, the absorption in the same region was numerically resolved into four bands, of which only the lowest

energy one (with the maximum at 12 300  $\text{cm}^{-1}$ ; see Figure 2) was integrated. This led to a small value of  $k_r = 2.6 \times 10^6 \text{ s}^{-1}$ . For the former case, the upper limit for the fluorescence quantum yield is  $3.7 \times 10^{-3}$ , well within the capabilities of the spectrofluorometer. For the latter case, however, it is only  $8.7 \times 10^{-5}$ , below the sensitivity of our instrument and thus consistent with the experimental observation that no fluorescence could be detected even at low temperature.

The  $S_0$ – $S_1$  energy gap in **1** and **2** is reduced by a quarter with respect to porphyrin and porphycene. According to the energy gap law,<sup>20</sup> this should increase the internal conversion rate by about 1 order of magnitude. Experimentally, a much larger enhancement is observed. Thus, the explanation of the rapid internal conversion process only in terms of the energy gap law is not sufficient, and other factors must be invoked. Efficient internal conversion from the  $S_1$  state has already been observed in various porphyrin derivatives<sup>21</sup> and assigned to nonplanarity of the structure. The same source for the photo-physical behavior may be postulated in the present case. The ground-state optimizations performed for **1** and **2** converge to “ruffled” or “domed” conformations. The crystal structure of **1** confirms that the molecule is nonplanar and has a “bowl-like” shape. On the other hand, **2** was found to be planar in the crystal, perhaps owing to intermolecular interactions. The differences in crystal structures obtained for two very similar molecules show that dibenzoporphycenes are rather floppy with respect to out-of-plane distortions. The lack of rigidity could enable the molecule to reach the region favoring the efficient  $S_1$  deactivation without a significant energy barrier.

Table 1 presents the results of calculations of the excited singlet states of **1** in both trans and cis tautomeric forms. An idealized, planar structure was assumed as a starting point (most geometry parameters, however, were taken from the X-ray data). Repeating the calculations for a bowl-like structure with exact X-ray geometry did not change the predicted absorption pattern much. Figure 4 presents the comparison between experiment and both sets of calculations. The agreement is quite satisfactory. Most important is the fact that, in accordance with the observations, the calculations predict more than two allowed transitions in the visible range. The cause of such behavior is that, contrary to porphyrin and porphycene, one of the low-lying excited states of **1** and **2** cannot be described in terms of the “four-orbital model”,<sup>22</sup> which takes into account only interactions between configurations involving the two highest occupied and two lowest unoccupied  $\pi$  orbitals. Since this procedure has been very popular and useful for comparing positions and shifts of electronic states in various porphyrin derivatives, we checked how well it works in the present case. The analysis of the CI matrix shows that the three allowed low-energy transitions of **1** (1, 2, and 4 of the trans form in Table 1) contain not only configurations involving the highest and second-highest occupied orbitals but also large admixtures of the fourth HOMO–LUMO, and even sixth HOMO–LUMO configurations. The magnitude of the squares of relevant CI coefficients may be used as a gauge of the Q or Soret band character of the computed transitions. As a measure of deviation from the four-orbital model, we define the coefficient  $r$ :

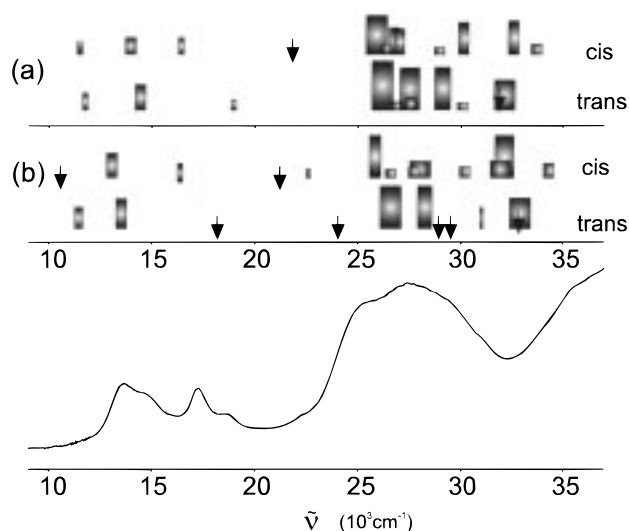
$$r = \frac{\sum_{i,j=1,2} C_{ij}^2}{\sum_{k,l} C_{kl}^2} \quad (1)$$



TABLE 1: INDO/S Calculated  $S_0-S_n$  Transitions for **1**

trans tautomer				cis tautomer			
	$E$ ( $10^3 \text{ cm}^{-1}$ ) <sup>a</sup>	symm <sup>b</sup>	leading config <sup>c</sup>		$E$ ( $10^3 \text{ cm}^{-1}$ ) <sup>a</sup>	symm <sup>d</sup>	leading config <sup>c</sup>
1	11.50 (0.11)	B <sub>u</sub>	0.67 (1 - 1)	1	11.52 (0.08)	B <sub>2</sub>	0.81 (1 - 1)
2	14.46 (0.30)	B <sub>u</sub>	0.69 (2 - 1)	2	13.97 (0.22)	A <sub>1</sub>	0.86 (2 - 1)
3	16.76 (0.00)	A <sub>g</sub>	0.96 (3 - 1)	3	16.39 (0.12)	B <sub>2</sub>	0.81 (3 - 1)
4	18.95 (0.06)	B <sub>u</sub>	0.85 (4 - 1)	4	21.77 (0.01)	B <sub>2</sub>	0.91 (4 - 1)
5	24.10 (0.00)	A <sub>g</sub>	0.84 (6 - 1)	5	23.37 (0.00)	A <sub>1</sub>	0.63 (5 - 1)
6	26.06 (1.16)	B <sub>u</sub>	0.68 (1 - 2)	6	25.78 (0.92)	A <sub>1</sub>	0.77 (1 - 2)
7	26.76 (0.10)	A <sub>u</sub>	0.91 (7 - 1)	7	26.30 (0.12)	B <sub>2</sub>	0.84 (8 - 1)
8	27.38 (0.95)	B <sub>u</sub>	0.53 (2 - 2)	8	26.63 (0.32)	B <sub>2</sub>	0.49 (1 - 3)
9	27.43 (0.15)	B <sub>u</sub>	0.51 (2 - 3)	9	26.76 (0.29)	A <sub>1</sub>	0.73 (7 - 1)
10	28.05 (0.00)	A <sub>g</sub>	0.71 (1 - 3)	10	28.79 (0.08)	A <sub>1</sub>	0.75 (2 - 3)
11	29.73 (0.00)	A <sub>g</sub>	0.63 (2 - 3)	11	28.96 (0.76)	B <sub>2</sub>	0.60 (1 - 3)
12	29.93 (0.09)	B <sub>u</sub>	0.66 (8 - 1)	12	29.96 (0.38)	A <sub>1</sub>	0.78 (3 - 2)
13	30.53 (0.00)	A <sub>g</sub>	0.58 (3 - 1)	13	30.10 (0.00)	B <sub>2</sub>	0.55 (6 - 1)
14	31.06 (0.00)	A <sub>g</sub>	0.70 (6 - 2)	14	31.27 (0.00)	A <sub>2</sub>	0.60 (6 - 2)
15	31.73 (0.01) <sup>e</sup>	A <sub>g</sub>	0.74 (9 - 1)	15	32.40 (0.40)	A <sub>1</sub>	0.75 (4 - 2)
16	31.98 (0.71)	B <sub>u</sub>	0.62 (8 - 1)	16	33.51 (0.13)	B <sub>1</sub>	0.81 (8 - 2)

<sup>a</sup> Oscillator strengths in parentheses. <sup>b</sup>  $C_{2h}$  assumed. <sup>c</sup> HOMO = 1, sHOMO = 2, LUMO = -1, sLUMO = -2, etc. <sup>d</sup>  $C_{2v}$  assumed, with  $z$  and  $y$  as in-plane axes. <sup>e</sup> Nonzero oscillator strength due to slight deviations from "ideal" symmetry.



**Figure 4.** INDO/S calculated energies of the lowest excited singlet states of **1**: (a) "idealized", planar structure (cf. Table 1); (b) bowl-like structure, corresponding to the X-ray geometry. The transitions with oscillator strength ( $f$ ) larger than 0.05 are indicated as bars, of which the area is proportional to  $f$ . Arrows mark transitions for which  $0.01 < f < 0.05$ . Transitions with  $f < 0.01$  are not shown. (Bottom) Experimentally measured absorption spectrum of **1** in acetonitrile.

The summation in the denominator occurs over all the singly excited configurations used by the program (in our case, 460 lowest energy ones). Actually, since the sum of squares of CI coefficients is normalized to 1, the value of  $r$  is obtained just from adding four terms in the numerator, which describe the four configurations used in the four-orbital model. By definition,  $r = 1.0$  if the four-orbital model (i.e.,  $2 \times 2$  basis) is used. When a large CI basis is applied, a value of  $r$  close to 1 indicates that a given transition is still well described by this simple approach.

We have calculated the values of  $r$  for the trans and cis forms of **1**, porphycene, and porphyrin. The results are shown in Table 2. For the trans form of **1**, the contributions of the four-orbital model configurations are 0.86, 0.96, and 0.24 for the first, second, and fourth calculated transitions, respectively. For the cis tautomer, the corresponding values are 0.72, 0.96, and 0.26 for the first, second, and third calculated transitions. Thus, the first two observed transitions of dibenzoporphycenes, lying at around 12 000 and 13 000  $\text{cm}^{-1}$ , respectively, may be safely considered as analogues of the Q bands of porphyrin and

TABLE 2: Values of  $r$  Calculated for Several ( $\pi\pi^*$ ) Excited Singlet States of **1**, Porphycene, and Porphyrin

1				porphycene				porphyrin			
trans		cis		trans		cis		trans		cis	
1 <sup>a</sup>	0.86	1	0.72	1	0.97	1	0.97	1	0.96	1	0.96
2	0.96	2	0.96	2	0.98	2	0.97	2	0.98	2	0.97
4	0.24	3	0.26	3	0.53	3	0.25	3	0.71	3	0.57
6	0.84	6	0.73	4	0.85	4	0.31	4	0.94	4	0.61
8	0.52	8	0.25	8	0.54	6	0.73			5	0.30
		11	0.34			8	0.53				

<sup>a</sup> Labeling refers to the  $n$ th lowest calculated excited singlet state.

porphycene, while the third, located around 17 000  $\text{cm}^{-1}$ , should be assigned to an "intruder" state.

For the UV transitions, the situation is more complicated. For the trans tautomer of **1**, the candidates for Soret bands are two transitions labeled 6 and 8 in Table 1. The  $r$  values are 0.84 and 0.52, respectively. Hence, only one of these transitions has a good counterpart in the four-orbital model. For the cis tautomer, the description in terms of four-orbital model is even worse. The only UV transition with approximately four-orbital character ( $r = 0.73$ ) is the sixth calculated excited state. Other transitions calculated in this region reveal  $r$  values of about 0.3. In other words, configurations from the four-orbital model are "spread" over several electronic transitions. It may be seen from Table 2 that such a pattern is not unique for **1**: porphycene and even the cis tautomer of porphyrin show similar behavior.

The reason that the low-lying excited states described by configurations from outside of the four-orbital model appear in **1** and **2** can be found in the topology. Dibenzoporphycenes can formally be obtained by adding two ethylene bridges to porphycene. Interaction of porphycene with the ethylene units leads to shifts of orbital energies, of which the magnitude and direction may be predicted from the properties of porphycene orbitals. The orbitals affected are those that have large LCAO coefficients at the positions of substitution and that possess symmetry appropriate for bonding or antibonding interactions. An example is provided by the LUMO of porphycene in both the trans and cis forms. The energy of this orbital energy should be lowered upon interaction with antibonding ethylene orbitals (Figure 5). The second LUMO, which has a very small electron density at the position of substitution, should practically not be affected. By the same mechanism, some occupied orbitals of porphycene will be destabilized after interaction with bonding ethylene orbitals. The positions of the two highest occupied

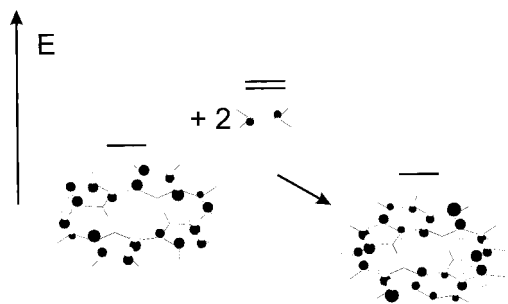


**Figure 5.** Illustration of energy stabilization of the LUMO of porphycene after bridging with two ethylene groups, which leads to dibenzoporphycene.

**TABLE 3: INDO/S Calculated Energies (in eV) of the Frontier Orbitals in 1, Porphycene, and Porphyrin**

	<b>1</b>		porphycene		porphyrin	
	trans	cis	trans	cis	trans	cis
-4	0.91	0.85	0.64	0.60	0.90	0.76
-3	-0.29	-0.29	0.16	0.17	0.02	0.09
-2	-1.02	-1.02	-1.16	-1.18	-1.58	-1.61
-1	-2.42	-2.39	-2.11	-2.09	-1.82	-1.78
1	-6.66	-6.65	-6.70	-6.73	-6.56	-6.63
2	-6.74	-6.79	-6.89	-6.87	-6.99	-6.94
3	-7.58	-7.43	-9.02	-8.95	-8.83	-8.80
4	-7.72	-7.99	-9.04	-9.04	-8.98	-8.92

orbitals remain unchanged, but their separation from lower lying ones becomes much smaller than in porphycene itself. Table 3 shows that in the trans form of **1**, the four highest occupied orbitals lie within the energy range of 1 eV, while for the corresponding tautomeric form of porphycene, the energy spacing between two pairs of highest occupied orbitals was larger than 2 eV. It is now clear that dominant configurations in the wave functions describing low-lying transitions will involve electron promotions from all four occupied orbitals. Inspection of Table 1 proves this is really the case.

In view of the above, it is quite remarkable that the low-lying electronic states of dibenzoporphycenes can still be very well described as analogues of the Q transitions of porphyrin and porphycene. We conclude that although the third observed transition in **1** and **2**, observed around 17 000 cm<sup>-1</sup>, corresponds to an "intruder" state, the first two transitions, located at around 12 000 and 13 000 cm<sup>-1</sup>, respectively, can be referred to as Q bands. Their energy separation, 1000–2000 cm<sup>-1</sup>, is quite similar to that observed in porphycene,<sup>4</sup> while the intensity ratio resembles that of porphyrin.

On the sole basis of calculations, it would not be possible to decide whether the observed spectra correspond to the cis or to the trans form, since quite similar absorption patterns are predicted for both tautomers (Figure 4). Moreover, the calculated ground-state energies of the two forms are also very close to each other. We think, however, that the observed lack of spectral response to the solvent polarity is a strong argument favoring the trans form, for which such behavior may be expected on the basis of the lack of a dipole moment in the planar form, or, at most, small dipole moment changes upon excitation in a nonplanar trans structure. In contrast, the calculated changes of the dipole moment upon excitation of the cis tautomer are very significant for several electronic transitions and should lead to readily observed absorption shifts. For instance, the dipole moment value calculated for the third lowest transition is 6.98 D, while that of the ground state is 0.87 D. The increase of dipole moment upon excitation is also predicted

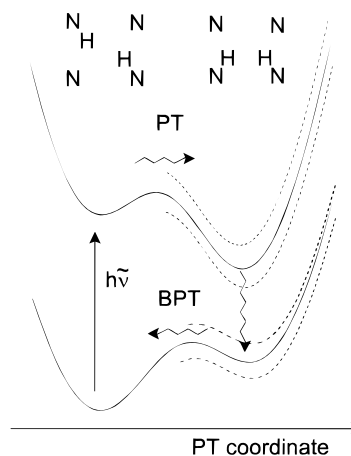


**Figure 6.** Schematic representation of radiationless deactivation involving cis-trans tautomerization: PT, proton transfer; BPT, back proton transfer. Dashed lines indicate energy changes of the cis form with varying degrees of planarity. Since they were calculated to be much stronger for the cis than for the trans structure, only the former are shown.

for several strong transitions in the UV range. Since no red shifts are observed in solvents of higher polarity, we conclude that the trans tautomers dominate the ground states of **1** and **2**, while the presence of cis as well as symmetrical forms is less probable. The situation is thus analogous to that observed in solutions of porphyrin and porphycene, even though the distance between the hydrogen-bonded nitrogen atoms is much smaller in both investigated dibenzoporphycenes.

The presence of cis tautomers in the excited state cannot be excluded, however. We have noticed an interesting result while calculating the excited-states pattern for nonplanar, domed, or ruffled structures of **1**. In the trans tautomers, the calculated transition energies were rather insensitive to the assumed geometry. On the other hand, the calculated S<sub>0</sub>–S<sub>1</sub> transition energy in cis forms strongly varied with changes in the input structure. For several geometries, the calculated excitation energies were much smaller than those of the trans tautomers. The source of different transition energies in the two tautomers was the fact that in the cis form a much stronger destabilization of the HOMO orbitals and stabilization of a LUMO orbital was observed upon variation of the molecular geometry.

This result suggests the interesting possibility of a radiationless deactivation of the lowest excited singlet state of the trans tautomer (Figure 6). After excitation, rapid proton transfer, followed by internal conversion and back proton transfer, would bring the molecule into the initial state. For such a case, the proton transfer coordinate would be strongly coupled to the low-frequency large amplitude vibrations, which effectively distort the molecule. Interestingly, for this mechanism to be efficient, nonplanarity is again a crucial factor, similarly as in the explanation of the fast internal conversion discussed before. This time, however, nonplanarity is just a prerequisite for a sequence of radiationless depopulation processes involving two chemical channels—proton shifts and a "purely" photophysical nonradiative step, S<sub>0</sub> ← S<sub>1</sub> internal conversion in the cis form.

It should be noted that the above mechanism of radiationless deactivation is unique for dibenzoporphycenes, since the stabilization of excitation energy in cis vs trans tautomers has its origin in the behavior of molecular orbitals involving the ethylene bridges. Further studies of the process could be based on custom-designed substituted dibenzoporphycenes, with a well-determined distorted geometry.

## Conclusions

Experimental and theoretical studies of two dibenzoporphycenes revealed both similarities and differences with respect to the parent compound. Structural changes caused by the ethylene bridges have an impact on both spectroscopy and photophysics. The absorption spectra are enriched, with respect to those of porphycene, by an appearance of an electronic transition lying between the analogues of Q and Soret bands. The latter correspond well to transitions observed in porphycene and porphyrin.

Modifications of the photophysics are much more pronounced. Very fast internal conversion is the only detectable process. It is attributed to the floppiness and possible nonplanarity of the molecules. Two different mechanisms involving nonplanarity are postulated to account for the rapid radiationless deactivation. First is a direct  $S_0 \leftarrow S_1$  transition. The second implies coupling between proton transfer and large amplitude vibrations. It should be noted that the two mechanisms may be interconnected.

The photophysical properties of **1** and **2** practically exclude their use in the area of photodynamic therapy, where other derivatives of porphycene show very good prospects. On the other hand, the same features that disqualify dibenzoporphycenes as potential phototherapeutic agents—lack of fluorescence, no population of the triplet state, and a very fast internal conversion—make them very promising candidates for applications in another fields, for instance, usage as polymer photostabilizers. An additional advantage in this respect is the absorption spectrum covering both visible and UV regions.

**Acknowledgment.** This work was supported by the Polish Committee for Scientific Research (Grant 3T01 128 01 08).

## References and Notes

- (1) Permanent address: Institute of Molecular and Atomic Physics, Academy of Sciences of Belarus, F. Scaryna Avenue 70, 220072 Minsk, Belarus.
- (2) Vogel, E.; Köcher, M.; Schmickler, H.; Lex, J. *Angew. Chem., Int. Ed. Engl.* **1986**, *25*, 257.

- (3) Vogel, E. *Pure Appl. Chem.* **1990**, *62*, 557. (b) Vogel, E. *Pure Appl. Chem.* **1993**, *65*, 143. (c) Vogel, E.; Koch, H.; Hou, X. L.; Lex, J.; Lausmann, M.; Kisters, M.; Aukaloo, M. A.; Richard, P.; Guillard, R. *Angew. Chem., Int. Ed. Engl.* **1993**, *32*, 1600.
- (4) Waluk, J.; Müller, M.; Swiderek, P.; Köcher, M.; Vogel, E.; Hohlneicher, G.; Michl, J. *J. Am. Chem. Soc.* **1991**, *113*, 5511.
- (5) (a) Waluk, J.; Vogel, E. *J. Phys. Chem.* **1994**, *98*, 4530. (b) Andersen, K. B.; Waluk, J.; Vogel, E. *Chem. Phys. Lett.* **1997**, *271*, 341.
- (6) (a) Aramendia, P. F.; Redmond, R. W.; Nonell, S.; Schuster, W.; Braslavsky, S. E.; Schaffner, K.; Vogel, E. *Photochem. Photobiol.* **1986**, *44*, 555. (b) Redmond, R. W.; Valduga, G.; Nonell, S.; Braslavsky, S. E.; Schaffner, K.; Vogel, E.; Pramod, K.; Köcher, M. *Photochem. Photobiol.* **1989**, *3*, 193. (c) Braslavsky, S. E.; Müller, M.; Mártire, D. O.; Pörting, S.; Bertolotti, S. G.; Chakravoti, S.; Koç-Weier, G.; Knipp, B.; Schaffner, K. *J. Photochem. Photobiol. B* **1997**, *40*, 191.
- (7) (a) Levanon, H.; Toporowicz, M.; Ofir, H.; Fessenden, R. W.; Das, P. K.; Vogel, E.; Köcher, M.; Pramod, K. *J. Phys. Chem.* **1988**, *92*, 2429. (b) Ofir, H.; Regev, A.; Levanon, H.; Vogel, E.; Köcher, M.; Balci, M. *J. Phys. Chem.* **1987**, *91*, 2686.
- (8) Vogel, E.; Köcher, M.; Lex, J.; Ermer, O. *Isr. J. Chem.* **1989**, *29*, 257.
- (9) Wehrle, B.; Limbach, H.-H.; Köcher, M.; Ermer, O.; Vogel, E. *Angew. Chem., Int. Ed. Engl.* **1987**, *26*, 934.
- (10) (a) Völker, S.; van der Waals, J. H. *Mol. Phys.* **1976**, *32*, 1703. (b) Radziszewski, J.; Waluk, J.; Nepraš, M.; Michl, J. *J. Phys. Chem.* **1991**, *95*, 1963.
- (11) Waluk, J.; Michl, J. *J. Org. Chem.* **1991**, *56*, 2729.
- (12) (a) Vogel, E. *Pure Appl. Chem.* **1993**, *65*, 143. (b) Donnerstag, D. Ph.D. Dissertation, University of Cologne, Germany, 1993. (c) Hübsch, U. Ph.D. Dissertation, University of Cologne, Germany, 1994.
- (13) Jasny, J. *J. Lumin.* **1978**, *17*, 143.
- (14) Dobkowski, J.; Grabowski, Z. R.; Jasny, J.; Zieliński, Z. *Acta Phys. Pol. A* **1995**, *88*, 445.
- (15) *Serena Software*; Bloomington, IN.
- (16) Stewart, J. J. P. *J. Comput. Chem.* **1989**, *10*, 209, 221.
- (17) Reynolds, C. H. *J. Org. Chem.* **1988**, *53*, 6061.
- (18) Ridley, J. E.; Zerner, M. Z. *Theor. Chim. Acta* **1973**, *32*, 111.
- (19) Strickler, S. J.; Berg, R. A. *J. Chem. Phys.* **1962**, *37*, 814.
- (20) Siebrand, W. *J. Chem. Phys.* **1967**, *46*, 440; **1967**, *47*, 2411.
- (21) (a) Gentenmann, S.; Medforth, C. J.; Forsyth, T. P.; Nurco, D. J.; Smith, K. M.; Fajer, J.; Holten, D. *J. Am. Chem. Soc.* **1994**, *116*, 7363. (b) Gentenmann, S.; Medforth, C. J.; Ema, T.; Nelson, N. Y.; Smith, K. M.; Fajer, J.; Holten, D. *Chem. Phys. Lett.* **1995**, *245*, 441. (c) Drain, C. M.; Kirmaier, C.; Medforth, C. J.; Nurco, D. J.; Smith, K. M.; Holten, D. *J. Phys. Chem.* **1996**, *100*, 11984. (d) Ravikanth, M.; Chandrasekhar, T. K. *J. Photochem. Photobiol. A* **1993**, *74*, 181. (e) Senge, M. O. *J. Photochem. Photobiol. B* **1992**, *16*, 3.
- (22) Gouterman, M. *J. Mol. Spectrosc.* **1961**, *6*, 138.